



Assessing the impact of measurement errors in the calculation of CWSI for characterizing the water status of several crop species

V. Gonzalez-Dugo¹ · P. J. Zarco-Tejada^{1,2}

Received: 11 March 2022 / Accepted: 10 August 2022
© The Author(s) 2022

Abstract

Canopy temperature is generally accepted as an indirect but rapid, accurate, and large-scale indicator of crop water status and is, therefore, proposed to monitor irrigation needs. Crop Water Stress Index (CWSI) is the most widely used among the existing thermal-based indicators, and its links with water stress have been demonstrated. When calculating CWSI using the empirical approach, the differential between canopy and air temperature is normalized by two thresholds, also known as baselines. The Non-water stress baseline (NWSB) in the empirical approach is calculated as the relationship between $T_c - T_a$ (°C) and the vapor pressure deficit (VPD, kPa) for well-irrigated crops. The baselines display different slopes depending on the species, which have a significant impact on the computed CWSI. This study analyzed the resulting errors on CWSI due to the measurement errors of critical inputs needed for its calculation. Six crop species were selected according to their NWSB with slopes that range from -0.5 to -3 °C·kPa⁻¹ and used for this analysis, assuming measurement errors ranging 0.2–1 °C for T_a , 0.25–2 °C for T_c , and 5–10% for relative humidity (RH). It was concluded that the effects observed on CWSI are heavily dependent on the slope of the NWSB and therefore vary across species. The calculation was very sensitive to the bias in air and canopy temperature. These errors were maximal as the slope of the NWSB was less steep. When the VPD ranged from 2 to 6.6 kPa, an error of 1 °C in measuring the air temperature affected CWSI between 28 and 83% in orange, which is the species displaying the minimum slope (-0.5 °C kPa⁻¹). On the contrary, crops with steeper baseline slopes such as squash (-3 °C kPa⁻¹) showed errors ranging between 2 and 8% for the same VPD interval. This differences among the different crops species considered in this study may be related to the contrasting coupling of the species to the atmosphere, that determines the influence of vapor pressure on the transpiration rate. This study highlights the importance of reliable climatic data and the need for accurate calibrated thermal sensors to calculate CWSI accurately.

Introduction

It is well accepted that canopy temperature is a sensitive indicator to estimate and monitor water status (Jackson et al. 1977). The relationships between heat dissipation, transpiration rate, and canopy temperature are well established (Gates 1968). The process of evaporation of water in the leaves consumes part of the energy from solar radiation and results in the cooling of transpiring leaves (Gates 1965). Water

stress causes partial stomatal closure and the reduction of plant transpiration rate (Jones 1999). As a consequence, the reduced evaporative cooling raises the leaf temperature in relation to ambient temperature. For this reason, canopy temperature has been used since the 1970s to assess crop water status (Jackson et al. 1977). Soon after the first studies dealing with canopy temperature, it was observed that it requires normalization according to the prevailing weather conditions. A given canopy temperature value as an indicator of water stress might differ depending on the concurrent ambient temperature. As a result, initial works dealing with the canopy temperature as an indicator of water stress identified the canopy-air differential ($T_c - T_a$) as an estimate of crop water status and, therefore, potentially useful for irrigation scheduling (Jackson et al. 1977).

In 1981, the group led by Idso and Jackson developed the Crop Water Stress Index (CWSI), which is the most currently used thermal-derived indicator to assess water status

✉ V. Gonzalez-Dugo
victoria.gonzalez@ias.csic.es

¹ Consejo Superior de Investigaciones Científicas (CSIC), Instituto de Agricultura Sostenible (IAS), Alameda del Obispo s/n, 14004 Cordoba, Spain

² School of Agriculture and Food (SAF-FVAS), Faculty of Engineering and Information Technology (FEIT), University of Melbourne, Melbourne, VIC, Australia

(Idso et al. 1981). In this index, the $(T_c - T_a)$ of a crop is normalized by two thresholds identified as the $(T_c - T_a)$ of a well-watered crop (lower limit, i.e., the NWSB) and a canopy where the stomata are entirely closed (upper limit, the line of maximum stress). As a result of this normalization, the index ranges from 0 (well-watered crops) to 1 (fully stressed crops). There are several ways to estimate CWSI, either empirical or analytical. For a complete review, see Maes and Steppe (2012). In the empirical approach, the lower limit is calculated from the Non-water-stressed baseline (NWSB), given by the linear relationship between the $(T_c - T_a)$ of a well-watered crop and the vapor pressure deficit (VPD; kPa). This relationship has been demonstrated to be stable for a given combination of crop and environment (Idso et al. 1984; Maes and Steppe 2012). Multiple NWSBs have been reported in the literature; see Idso (1982) for a list of some NWSBs for the most important crops and Maes and Steppe (2012) for an updated list. In their work published in 1981, Idso and coworkers developed a methodology to estimate the upper limit based on the NWSB, which is currently used for the CWSI calculation (Irmak et al. 2000; Testi et al. 2008; Taghvaeian et al. 2012). In conclusion, the data input of the CWSI calculation using the empirical approach is limited to T_c , T_a , VPD, and the coefficients of the NWSB. Alternative methodologies to estimate the CWSI include the assessment of the temperature of dry and wet references that can be measured either directly from leaves (Jones et al. 2002; Leinonen and Jones 2004) or from reference surfaces (Maes et al. 2016; Apolo-Apolo et al. 2020).

Initially, T_c was measured using hand-held thermometers that pointed directly at the vegetation canopy, as described in Idso and coworkers' studies (Idso et al. 1981). Currently, different sensors can be used to estimate canopy temperature, being the IRT sensors installed over the canopy and thermography, the most widely used (Sepulcre-Canto et al. 2006). The IRT sensors are well suited to monitor T_c continuously and especially to detect the temperature range of well-watered plants needed for the NWSB assessment. Thermography has experienced remarkable progress in the last decades related to improved technology and sensor development. These advances have been particularly relevant when the main objective is the assessment of the spatial variability of T_c , either within tree crowns (Gonzalez-Dugo et al. 2012) or in field crops, as is required in the context of precision agriculture (Meron et al. 2010). Remote sensing of temperature enables the monitoring of large surfaces, and its incorporation as inputs into energy balance models has successfully being used to estimate evapotranspiration (Allen et al. 2007). Thermal sensors onboard aircrafts or drones are required for the monitoring of discontinuous canopies (such as orchard tree crops) due to the high-spatial-resolution imagery needed to target tree crowns,

while avoiding soil background and shadow effects. There is a wide range of thermal cameras available for this purpose, such as the uncooled thermal cameras widely used in agricultural applications because of their lightweight, low power consumption, and price (Zhao et al. 2018). On the other hand, cooled cameras are more sensitive and accurate, although their use is not always feasible due to weight, dimensions and power supply restrictions, especially when installed onboard drones. In most situations, miniaturized uncooled thermal cameras are not calibrated, or the calibration is generic, and therefore, the range of error in the absolute temperature assessment increases. Berni et al. (2009b) observed an RMSE before and after calibration of about 3.4 and 0.9 K, respectively. Zhao et al. (2018) quantified the error in temperature associated with stitching during the mosaic generation and observed that it remained below 1 °C.

Similarly, the accuracy in measuring the environmental conditions used to calculate CWSI (i.e., T_a and RH) or any other thermal-derived water stress indicator, such as I_g or I_3 (Jones 1999), must also be considered. The reliability of weather stations and the relevance of accurate data are paramount and not always considered. In most cases, weather data are collected from available meteorological stations, sometimes far from the study site. National agencies usually display a net of stations covering most of the regions of interest, with a variable set of measurements that often include air temperature and relative humidity, both inputs required to compute CWSI empirically. The World Meteorological Organization (WMO) publishes a series of guides of good practices and procedures in meteorological measures that serve as a framework for the standardization of meteorological observations. The maximal allowable distance to a weather station must be valued for each case, according to the landscape. Comparisons performed in Brazil (Lopes et al. 2021) and New Zealand (Mason et al. 2017) among national and independent weather stations demonstrated that, for such climatic conditions, air temperature and solar radiation were well correlated within a distance below 20 km, while relative humidity and rainfall seemed to be more affected by local variations. Other climatic conditions might differ from these trends. There is an increasing trend for growers to install on-site automatic weather stations to address the distance issue, which provides more accurate localized weather, but these stations need regular calibration and maintenance to provide accurate data (Lopardo et al. 2015).

Because of the increasing interest and ease of use in the CWSI calculation to estimate crop water status, it is critical to assess the different sources of error yielding inaccuracies. The overall objective of this paper was to determine the range of error in the CWSI calculation associated with the inaccuracies of the three most important inputs required for

the empirical model generally used in remote sensing and precision agriculture, i.e. canopy temperature, air temperature and the relative humidity.

Materials and methods

Six species were selected for this study: three orchard tree crops (almond, mandarin, and orange) and three herbaceous crops (turfgrass, maize, and squash). The NWSB were calculated experimentally using the relationship between the differential of the air and canopy temperature ($T_c - T_a$, °C) and the vapor pressure deficit (VPD, kPa) under well-watered conditions. The NWSBs were developed in Spain and USA

Table 1 Species considered in this study. The slope (m) and intercept (b) of the NWSB are reported, together with the research location and the reference

Species	m	b	Location	Reference
Orange	-0.38	4.59	Southern Spain	Gonzalez-Dugo et al. (2014)
Mandarin	-0.50	4.06	Southern Spain	Gonzalez-Dugo et al. (2014)
Almond	-1.21	3.42	Southern Spain	Gonzalez-Dugo et al. (2019)
Turfgrass	-0.86	4.70	Georgia (USA)	Carrow (1989)
Maize	-1.97	3.11	Arizona (USA)	Idso (1982)
Squash	-3.09	6.91	Arizona (USA)	Idso (1982)

(Table 1). The selection of species was made to account for a large range of slopes, ranging from -0.38 °C·kPa $^{-1}$ in orange to -3.09 °C kPa $^{-1}$ in squash. The slopes and intercepts of the NWSBs used in this study can be observed in Table 1.

Climatic data

The climatic dataset used for this analysis was derived from actual pairs of T_a and RH hourly values measured at three different locations: Seville (37.8° N, 5.4° W; Southern Spain), nearby the location where the citrus and almond crops were studied, Maricopa (33.4° N, 112.0° W, Arizona, USA), and Griffin (33.1° N, 84.1° W, Georgia, USA). Mean 1-h values around noon during July on cloudless days were used in the three cases. The two variables were related, as shown in Fig. 1A–C. The lower and upper boundaries were determined by calculating the 5% and 95% quantile regression, respectively, and correspond to the thresholds containing the typical T_a –RH values observed for each site. Using 1 °C T_a and 1% RH steps, every possible combination within the boundaries was identified, as shown in Fig. 1D–F for the three locations. All the cases analyzed resulted in VPD values that ranged from 0.94 to 6.64 kPa in the case of Southern Spain, from 1.84 to 7.38 kPa in Arizona, and from 0.32 to 4.65 kPa in Georgia. The use of CWSI is not recommended for VPDs below 2 kPa, because of the low levels of the signal: noise ratio within this range (Testi et al. 2008). Therefore, the study was focused on VPD values higher than 2 kPa.

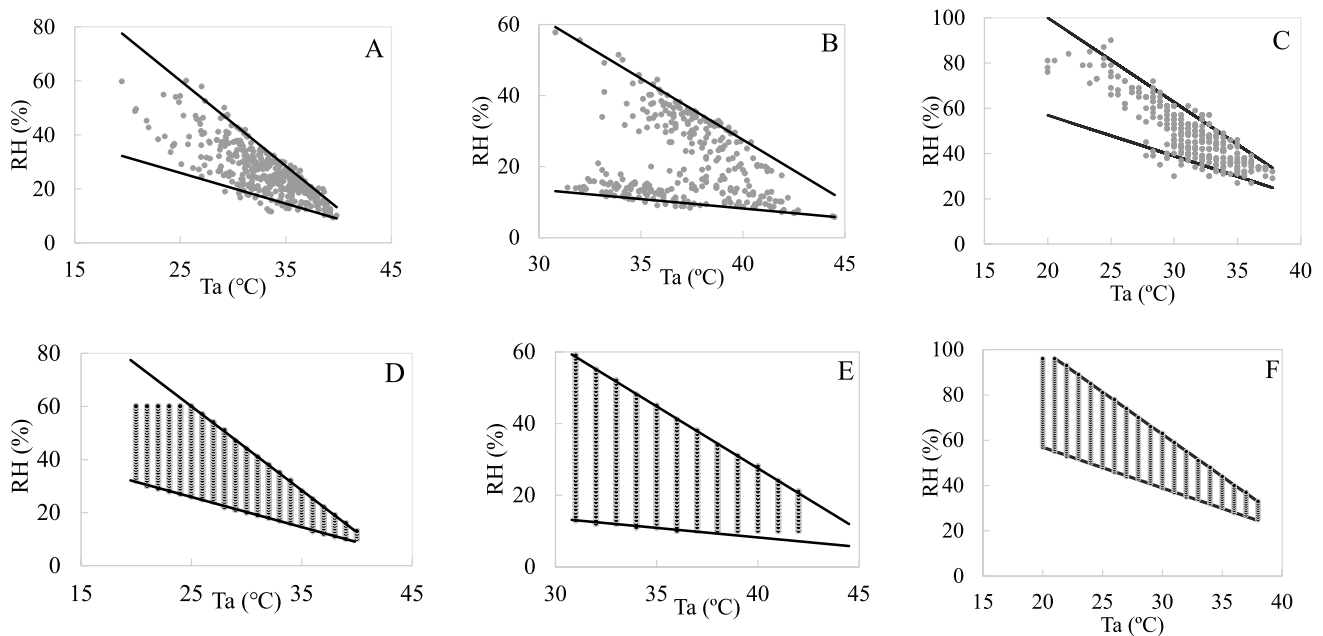


Fig. 1 Databases of T_a vs. RH for actual values measured in Seville, Spain (A), Arizona, USA (B), and Griffin, USA (C). Black lines identified the 5% and 95% quantile regressions for each dataset. D–F

identified the number of cases considered for each study case (526, 395, and 501 cases for Spain, Arizona, and Georgia, respectively), resulting from combining 1 °C T_a and 1% RH steps within boundaries

Analysis of the sensitivity of CWSI to meteorological weather data

According to the Guide to Agricultural Meteorological practices, published by the World Meteorological Organization (WMO 2010), the minimum accuracy recommended for air temperature, and relative humidity is ± 0.2 °C and $\pm 5\%$, respectively. These values were chosen as thresholds to analyze the sensitivity of the CWSI calculation to the concerned meteorological variables. As a result of the combinations of the accuracies in both inputs, four cases were evaluated, corresponding to the following scenarios (expressed as variation in T_a /variation in RH): (i) $+0.2$ °C/ $+5\%$, (ii) $+0.2$ °C/ -5% , (iii) -0.2 °C/ $+5\%$ and (iv) -0.2 °C/ -5% . Therefore, for each pair of T_a and RH values indicated in Fig. 1D–F, the four combinations were calculated, and the average and standard deviation were analyzed.

Because the distance to the weather station and differences in the prevailing environmental conditions might increase the range of variation, the error in CWSI associated with a more significant deviation in the meteorological data was calculated. For this reason, the bias was increased to ± 1 °C in the air temperature and $\pm 10\%$ in relative humidity. Therefore, the effect of these biases was computed separately for each input.

Analysis of the sensitivity of CWSI to inaccuracies in T_c determination

The overall effect of inaccuracies in the T_c determination on the calculation of the CWSI was evaluated. The selected T_c deviation ranged between 0.25 and 2 °C, using a 0.25 °C-step for each pair of T_a and RH values shown in Fig. 1D–F. Special attention was paid to a value of 1 °C, as it is the threshold often considered admissible in operational applications.

Analysis of the sensitivity of CWSI to the combined inaccuracies of T_c and climatic data

Finally, the combined effect of inaccuracies in weather inputs and T_c in the CWSI calculation was evaluated. The same values analyzed in the previous sections were used in this study (i.e., 1 °C and 10% error in T_a and RH, respectively, and 1 °C in T_c). The combination of the three values resulted in eight cases evaluated for each crop ($+T_a/+RH/+T_c$, $+T_a/-RH/+T_c$, $+T_a/-RH/-T_c$, $+T_a/+RH/-T_c$, $-T_a/+RH/+T_c$, $-T_a/-RH/+T_c$, $-T_a/-RH/-T_c$, $-T_a/+RH/-T_c$). The objective of this analysis was to combine the results assessed before quantifying the overall inaccuracy expected when all errors were combined.

A final assessment using real data was carried out with an almond dataset obtained from 2014 to 2015 to analyze the

influence of these errors in CWSI inputs on the relationship with physiological measures. Temperature data over well-watered and water-stressed almond trees were registered continuously using four IRT sensors with an angular field of view of 44° (Model IRR-P, Apogee Instrument Inc., Logan, Utah, USA) mounted on masts installed over the trees, targeting the crowns in a 45° zenith angle and 0° azimuth (i.e., facing the canopy exposed to south). The temperature values acquired over well-watered trees were used to derive the NWSB, which serves as a basis for calculating the CWSI in the four monitored trees. In addition to this, in eight days during the 2014 and 2015 field campaign, the stomatal conductance was measured using a porometer (model SC-1, Decagon Devices, Washington DC, USA). More information can be found in Gonzalez-Dugo et al. (2019).

Results

Assessment of the CWSI uncertainty due to atmospheric characterization

When the accuracy levels provided by the WMO in air temperature and relative humidity measurements were combined, the error in the calculation associated with the accuracy of weather station data ranged between 0 and 17% (Fig. 2A, B). The dataset was split between trees (Fig. 2A) and herbaceous crops (Fig. 2B). It can be observed that the percentage of variation was maximal for orange which displayed mean values ranging between 17 and 6% when the VPD increased from 2 to 6.6 kPa, respectively. In the case of mandarin and almond, mean values for a VPD equal to 2 were 12% and 6%, respectively (Fig. 2A). As happened in the case of orange, the relevance of the accuracy in meteorological data decreased as VPD increased. In the case of herbaceous, the error associated was smaller than 10% and displayed similar behavior to what was observed for the tree crops (Fig. 2B), i.e., a decreasing relevance of the error associated as the VPD increased. Squash was the crop showing minimum values. The range of variation oscillated between 1.8 and 2.7% for the VPD values considered in this study. The differences among the species considered were related to the slope of the NWSBs, as observed in Fig. 3. The coefficient of the power adjustment (corresponding with the %variation for a VPD value equal to 1) was closely correlated with the slope of the NWSB (detailed in Table 1).

Assessment of the uncertainty in CWSI associated with micro-climatic variability

The distance and representativeness of any standard weather station for a given crop affecting the accuracy of the CWSI calculation were evaluated. The spatial variability of air

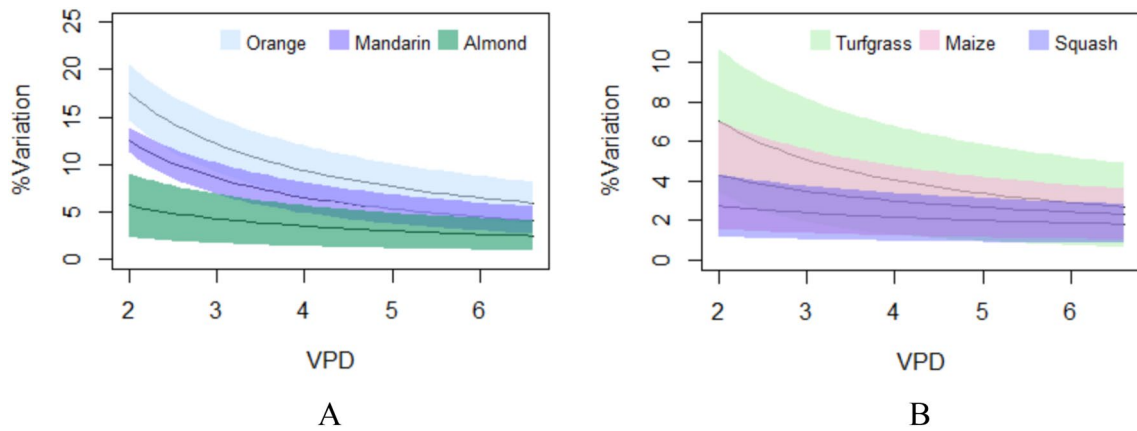


Fig. 2 Analysis of the error in the CWSI calculation associated with a combined inaccuracy of $\pm 0.2\text{ }^{\circ}\text{C}$ in T_a and $\pm 5\%$ in RH for the tree crops (orange, mandarin, and almonds, **A**) and herbaceous crops (tur-

grass, maize, and squash, **B**). The six species were computed separately. For each species, the line represented the average value, and the shaded area indicated the standard deviation

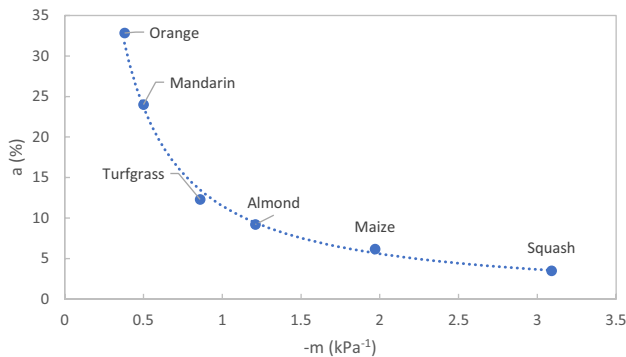


Fig. 3 Relationship between the coefficients of the power functions described in Fig. 2 (a ; %) adjusted for each crop and the slope of the NWSB ($-m$). The crop was identified for each point

temperature and relative humidity depends on multiple factors, such as topography, orientation and prevailing wind direction. As observed before, the relevance of the errors in the determination of T_a and RH was species dependent. When the two errors were computed separately, it was observed that the effect of inaccuracies in air temperature was more significant compared to the relative humidity (Figs. 4 and 5). Moreover, the effect associated with T_a diverged across species, according to the slope of the NWSB (Fig. 4). The relevance of the CWSI value on the % variation associated with T_a was moderate; therefore, values plotted in Fig. 4 averaged all the CWSI. Figures S1A to S1F in the supplementary material showed the % variation for each crop identifying the CWSI-family curves.

In the case of the RH, the % of error was significantly smaller and ranged from 0 to 12% (Fig. 5). In contrast with

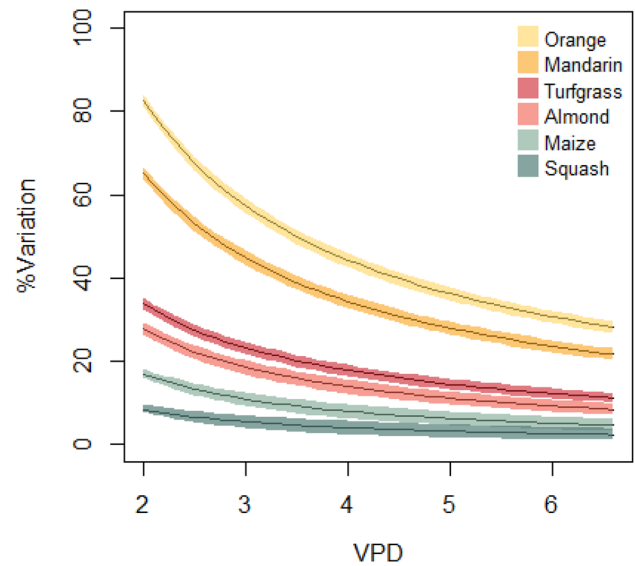


Fig. 4 Analysis of the CWSI calculation error associated with an inaccuracy of $\pm 1\text{ }^{\circ}\text{C}$ in T_a . The six species are computed separately. For each species, the line represents the average value, and the shaded area indicated the standard deviation

the finding in T_a , the range of errors was similar for all the species considered. Because of the contrasting behavior displayed by orange and squash in the previous section, these species are presented in Fig. 5A, B. The effect of the CWSI value in the % variation associated with an error in RH was significant (Fig. 5); maximum values were observed for low CWSI and decreased as the index increased from 0.1 to 0.9. When CWSI was equal to 1, the error was 0. The complete dataset for the six species can be found in Figures S2A to S2F.

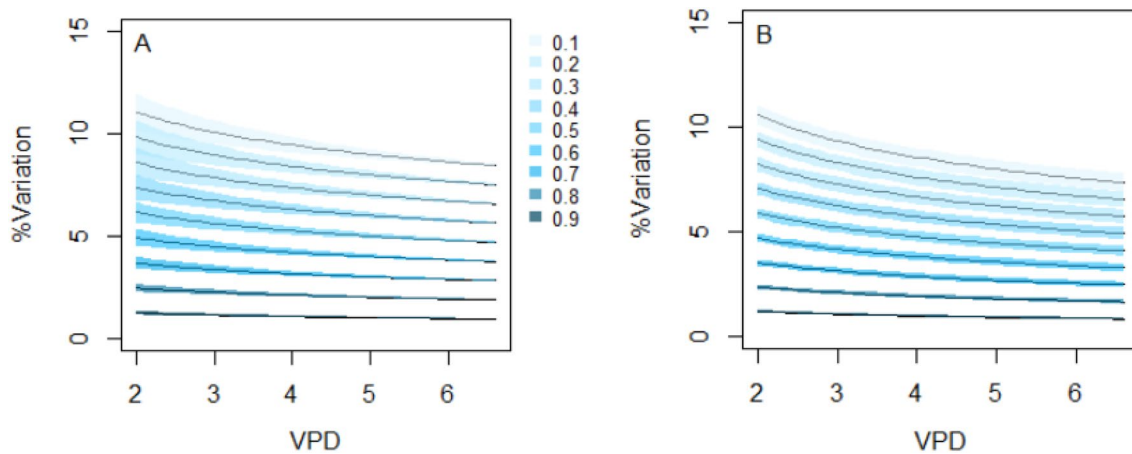


Fig. 5 Analysis of the CWSI calculation error associated with an inaccuracy of $\pm 10\%$ in RH in orange (A) and squash (B) identifying the values for each CWSI. For each CWSI, the line represented the average value, and the shaded area indicated the standard deviation

Assessment of the uncertainty in the CWSI calculation associated with inaccurate canopy temperature measurements

The effect of inaccuracies in determining T_c was of the same order of magnitude as T_a . Figure 6 plots the % of error for each species according to the VPD value and the error in the estimation of T_c , from 0.25 to 2 °C. White horizontal lines identified the effect in the CWSI calculation associated with an error in the T_c estimation of 1 °C. As happened before, errors were species-dependent and increased as the slope of the NWSB decreased. Therefore, orange displayed the largest errors among all the species considered in this study. For a bias in T_c determination of 1 °C, the error ranged between 29 and 88% for VPD values considered. Squash was the species displaying minimal errors, ranging from 3 to 8%.

Assessment of the uncertainty in CWSI due to the combined effects of ambient conditions and canopy temperature retrieval

The combined effects of ambient and canopy temperature were considered due to the confounding interaction of both inputs under real conditions. The inaccuracy associated with the climatic variables is wide if the influence of distance and topography is considered on the representativeness of the weather station for a given plot. Eight cases were tested for each species, resulting from combining ± 1 °C T_c , ± 1 °C T_a , and $\pm 10\%$ RH variations. As expected, the crops ranked according to the slope of the NWSB (Fig. 7). For each crop, two families of curves can be observed. The first family of curves was dominated by T_a and T_c combinations with additive effects. As these two variables enter the calculation as $T_c - T_a$, the additive errors corresponded to $+T_a / -T_c$ and $-T_a / +T_c$ combinations. In comparison, the effect of RH was

relatively small. The second set of curves displayed values close to 0 and related to the cases where the error in T_c and T_a compensated each other.

In the case of orange, maximum values ranged from 150 to 200% for VPD equal to 2 kPa, and 60–70% for VPD value equal to 6.6 kPa (Fig. 7A). Again, squash displayed minimum values lower than 25% for any curve and VPD considered (Fig. 7F). The rest of the crops showed intermediate behaviors between these two extremes.

Analysis of the effect of the error in CWSI inputs on the relationship with physiological variables

An almond dataset obtained from 2014 to 2016 (Gonzalez-Dugo et al. 2019) was used to observe whether the errors in CWSI described in this study affect the relationships with physiological variables. VPD values for this dataset ranged from 1.93 to 4.22 kPa, with a mean value of 2.92 kPa. Figure 8 shows the relationship between CWSI and the stomatal conductance for the original dataset, the CWSI considering an error of +1 °C in T_c , or +10% in RH. The effect associated with T_a was not included as it was similar to T_c . It can be observed that a good correlation was maintained and that the R^2 never decreased below 0.86. As the effect of increasing 1 °C in T_c was only slightly affected by the actual CWSI value (as shown in Figure S1), the relationship showed a lateral displacement, meaning that the main change was related to the absolute values. The relationship with stomatal conductance was maintained, but the shift showed that a given CWSI value corresponded to a change of approximately 70 mmol/m²/s. On average, this error in T_c resulted in the increase of CWSI in 0.18 compared to the original values. In the case of a +10% error in RH, the effect was more significant for low CWSI and close to 0 for high CWSI values, which agreed with results presented in Figs. 5 and

S2. On average, the resulting CWSI was 0.08 lower than the original value.

Discussion

Species strongly differ in transpiration response to environmental constraints, even under well-watered conditions. It has been demonstrated that citrus display low transpiration rates, even under well-watered conditions (Veste et al. 2000; Villalobos et al. 2009). However, when different experiments and locations are compared, the NWSBs might differ, even for the same species. This difference is related to the cultivar selection and the prevailing environmental conditions. Previous works demonstrated the difficulty of monitoring water status in citrus using canopy temperature (Gonzalez-Dugo et al. 2014). The limitations were associated with temperature oscillations probably related to stomatal fluctuations (Dzikiti et al. 2007) and the contrasting behavior of new leaves in the vegetative flush growth. In citrus, canopy temperature readings must be handled thoroughly for monitoring the water status.

Previous studies have shown the sensitivity of thermal-derived indices to other weather variables, such as solar radiation or wind speed (Jones 1999; Agam et al. 2013). Maes and Steppe (2012) analyzed the variation in climatic inputs on the transpiration rate and the canopy temperature. This study focused on the effect of the inaccuracies in determining the variables included in the empirical formulation of CWSI. It is conceived as a theoretical analysis based on the systematic variation of the identified inputs.

It can be concluded that the slope of the NWSB severely determines the overall effect of inaccuracies in the input values on the overall CWSI calculation. This effect can be related to the differences among the crops in the coupling to the atmosphere. The Penman–Monteith equation describes how the evaporation is affected by the climatic and crop factors and is expressed as follows:

$$LE = \frac{\Delta(R_n - G) + \frac{\rho C_p}{r_a} VPD}{\Delta + \gamma \left(1 + \frac{r_s}{r_a}\right)}, \quad (1)$$

where LE correspond to the latent heat flux, Δ is the slope of the saturation vapor pressure vs temperature relationship, R_n and G are the net radiation and soil heat flux respectively, ρ is the air density, C_p is the specific heat of air at constant pressure, r_a and r_c are the aerodynamic and canopy resistance, respectively, and γ is the psychrometric constant.

The crops with low height, large leaves and smooth closed canopies (such as squash) are decoupled from the atmosphere, and the aerodynamic resistance is very high. Under these circumstances, the evaporation is close to

the equilibrium rate and is related, mainly, to the radiation receipt, at least until severe water stress intervenes (Jarvis 1985). Therefore, the effect of VPD is of much lesser importance than in the case of very coupled canopies, because of the feedback between the transpiration rate and the local saturation deficit around the leaves. Tall and rough canopies, on the contrary, have negligible aerodynamic resistance (compared to the canopy resistance). In this case, the transpiration is close to the imposed evaporation, where the transpiration is largely set by the VPD values (Jarvis 1985). In conclusion, the higher coupling to the atmosphere, the larger the effect of VPD and, therefore, the larger the effect of its inaccuracies. Turfgrass was the only species that seems to not follow this premise. The NWSB chosen for this study ($T_c - T_a = 4.70 - 0.86 \cdot VPD$) displayed a smoother slope compared to other turfgrass species studied in the same experiment, and elsewhere (see the list gathered by Maes and Steppe 2012). In this list, the slopes for turfgrass varied between -1.25 and -2.46 , which seemed to better align with the hypothesis presented here. In any case, we have disregarded the effect of the different climatic conditions on the slope, which may also have an influence on the absolute values of the contrasted formulations for the same crop that can be found in the literature.

The most relevant input was the temperature, either T_c or T_a . For example, for an error of ± 1 °C in T_a , the effect in orange ranged between 28 and 82%, depending on the VPD value; while it reached between 2 and 8% in squash. The impact of the relative humidity was of lesser importance and the same order among all the species considered (1–15%). There are two reasons for this effect. First of all, the propagation of errors in RH in the VPD calculation is of lesser importance, compared to errors in T_a . The analysis of varying T_a and RH within a range of ± 4 °C and $\pm 4\%$, respectively, can be observed in Figure S3. A deviation of 1% in RH resulted in a change of VPD between 1 and 2%. Nevertheless, a deviation of 1 °C in T_a resulted in a change between 5 and 6%.

The second reason is associated with the calculation of the CWSI. Figure 9A, B shows the magnitude of the deviations in 1 °C T_a , 1 °C T_c , and 10% RH for a single point, as example in orange and squash. In the case of orange, the magnitude of the changes was significant compared to the difference between the upper and lower limits. On the contrary, these variations were minor compared to the thresholds established for squash.

The relevance of correct calibration procedures cannot be overemphasized. Comparing one IRT sensor and two thermal cameras, Aragon et al. (2020) observed that measurement bias and vignette effects were greatly reduced in both imagers, resulting in a RMSE of 1 °C or less. Although the imagers displayed significant differences between them

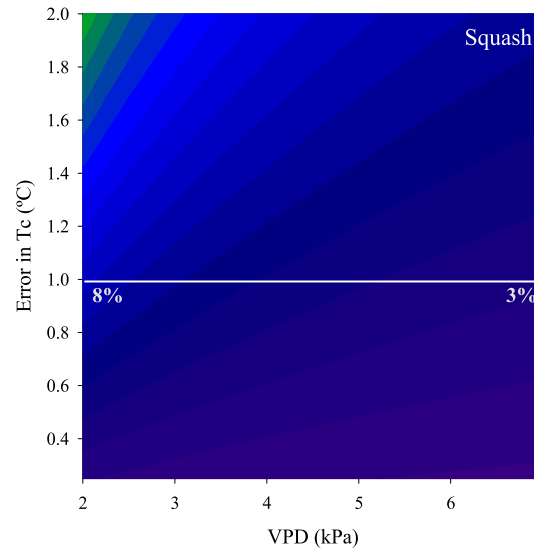
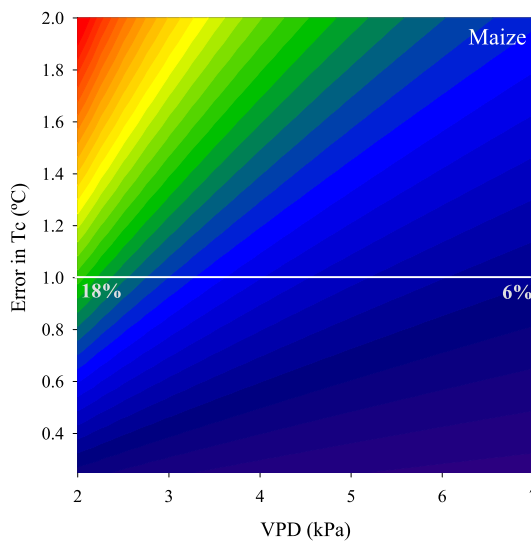
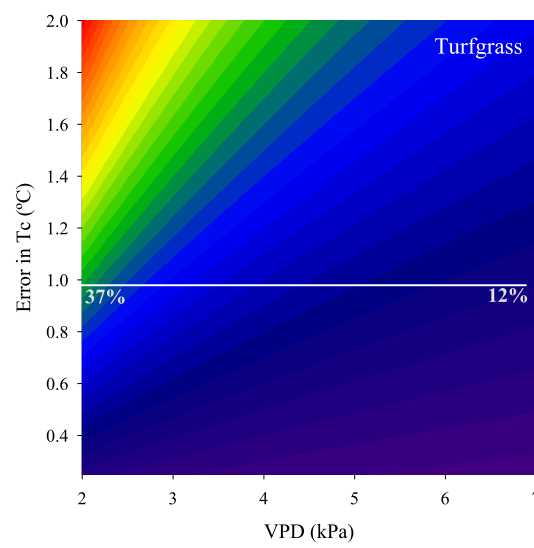
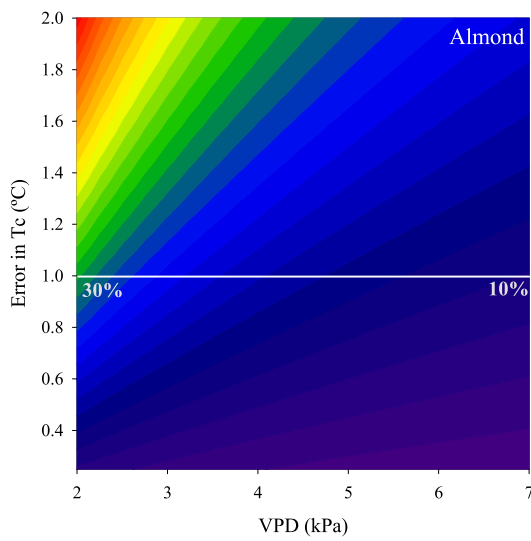
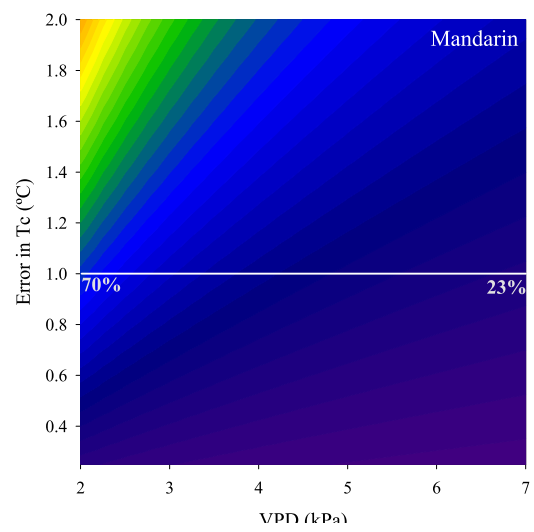
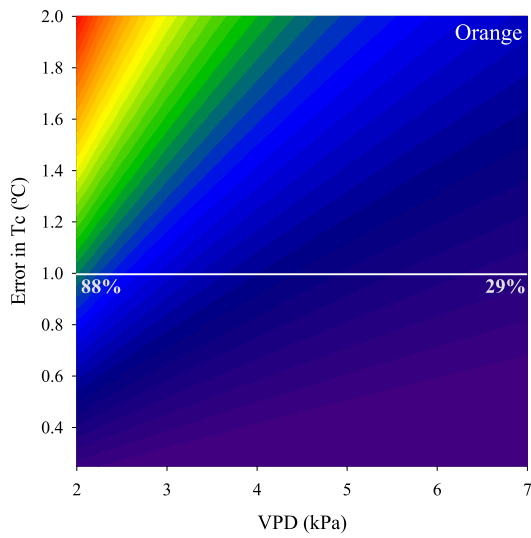


Fig. 6 Contour plot representing the overall effect on the CWSI calculation for VPD ranging from 2 to 7 kPa (X -axis) and an error in T_c calculation ranging from 0.25 to 2 °C (Y -axis). White horizontal lines identify the results obtained for an error in T_c estimation of 1 °C, which is the common efficiency goal in most scientific studies (Berni et al. 2009b; Aragon et al. 2020). The two values in white for each figure indicate the variation in CWSI associated with an error in T_c of 1 °C and for VPD values of 2 and 7 kPa, respectively. It is important to stress that scales are different for each row; left and right figures share the same legend

before calibration, the method developed in this work enabled more accurate surface temperature retrievals.

Moreover, the pattern of change of the three inputs considered can be observed. The error in the estimation of the relative humidity was associated with a lateral displacement of the value compared to the original departure point. This movement slightly affects the distance between the two thresholds. The error of 1 °C in the estimation of canopy temperature resulted in the vertical displacement of the value. According to the difference between the upper and the lower limits, this can be very relevant (as observed in Fig. 9A for orange) or not (as in the case of squash, Fig. 9B). Finally, the error of 1 °C in the determination of T_a produced a diagonal displacement due to its implication in both, $T_c - T_a$ and VPD calculations. In any case, the effect is dominated by vertical displacement. Similar results were observed by Poirier-Pocovi and Bailey (2020) when the sensitivity of the temperature of a leaf wet (T_{wet} , a simplification method to calculate the lower limit) to weather conditions was assessed.

In a previous paper, Idso et al. (1990) analyzed the influence of site location for air temperature and relative humidity measurements for estimating the NWSB in the case of bell pepper. They used an NWSB equal to $(T_c - T_a) = 2.35 - 1.87 \cdot \text{VPD}$ and compared the differences among the slope and intercept values when the weather data were obtained from several psychrometers placed in four different locations, inside and outside the canopy, close to the study site and 4 km away. They found minor variations in the NWSB definition when the four weather locations were compared. To analyze the generality of their results, they related the behavior of bell pepper with synthetic NWSBs built using maximum and minimum values published elsewhere (Idso 1982). They observed that the differences among the different locations were minimal for a

slope coinciding with that of bell pepper (-1.9 °C kPa^{-1}) and increased for lower and higher values. They argued that this slope value was very similar to the slope of the relationship between VPD and air temperature for these locations, which might explain the slight difference observed in the case of bell pepper. Although their analysis was focused on the NWSB computation while this study is focused on the CWSI calculation, a similar behavior might be expected as the theoretical background is closely related. On the contrary, their result contrasted with this study. In this case, the pattern was a continuous decreasing trend as the slope increased, as is depicted in Fig. 3. The use of synthetic crops instead of actual values might be at the origin of this discrepancy.

This study quantified the relevance of these errors in computing CWSI in absolute terms. In any case, the relationship with physiological measures was significant when systematic errors were introduced and still yielded good results.

What are the implications of these results in the practical application of the CWSI? In most crops, especially those with a steeper NWSB, the error associated with the inputs was relatively small, although the range of uncertainty observed in this study must be considered. Special attention must be paid especially to those crops with a least steep slope, such as citrus, or other crops well adapted to drought, such as olives (Berni et al. 2009a). In those cases, the proximity of well-calibrated weather stations and accurate canopy temperature measurements becomes essential to developing any practical application of CWSI. Strong efforts must be invested to optimize data quality when the thermal-derived indices are used concerning climatic data and accurate calibrated thermal sensors.

Conclusions

This study quantified the magnitude of the effect of errors in data input on the CWSI calculation is crop-dependent, and demonstrated that it depends on the slope of the NWSB. In this study, those crops displaying a less steep slope, such as citrus, show more significant effects on the overall CWSI computation. These are species coupled to the atmosphere where the transpiration is largely affected by the VPD values. In contrast, this effect was moderate in those species displaying a steeper slope, such as squash, as differences

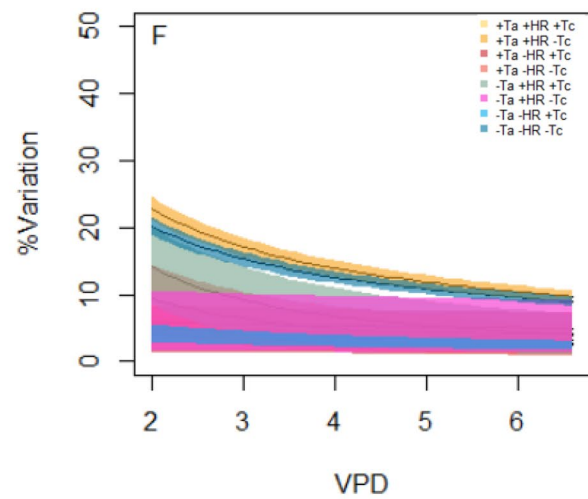
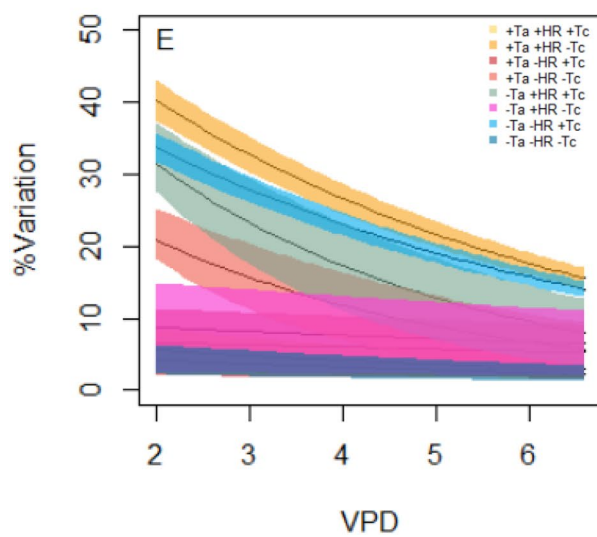
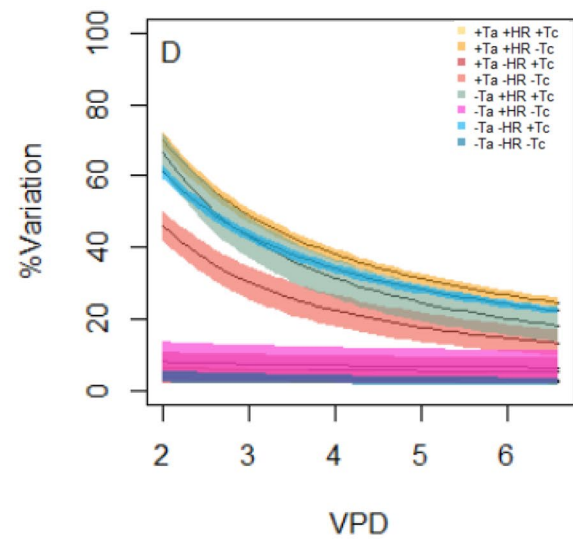
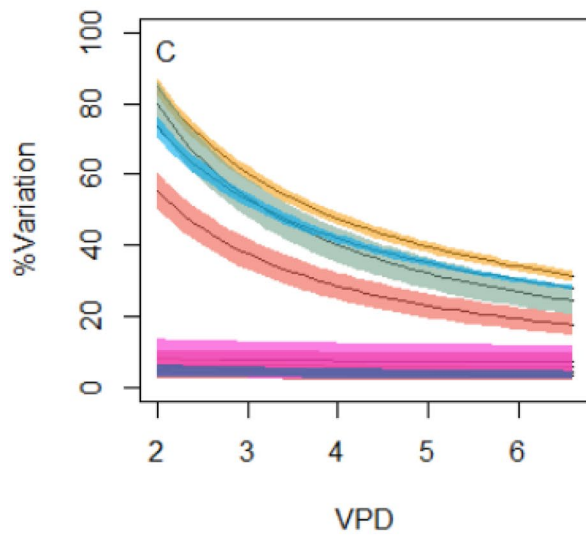
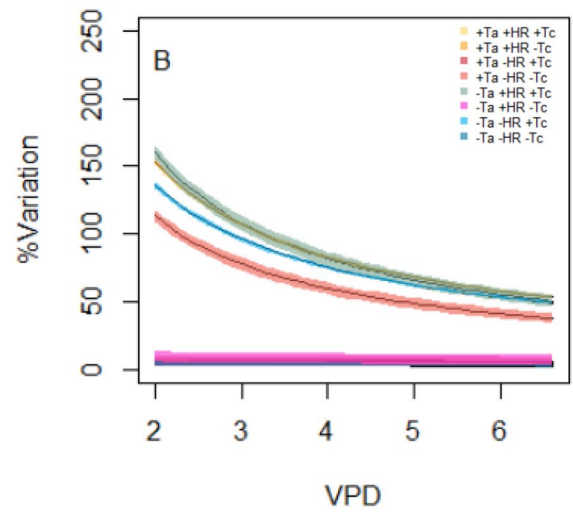
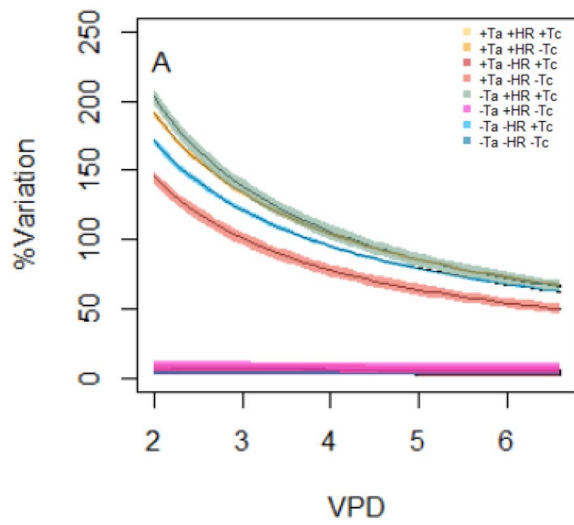


Fig. 7 Analysis of the error in the CWSI calculation associated with an inaccuracy of $\pm 1\text{ }^{\circ}\text{C}$ in T_a and T_c , and $\pm 10\%$ in RH, for orange (A), mandarin (B), turfgrass (C), almond (D), maize (E) and squash (F). The continuous line represented the average value, and the shaded area indicated the standard deviation. For each species, the eight cases resulting from the combination of the three factors considered are included

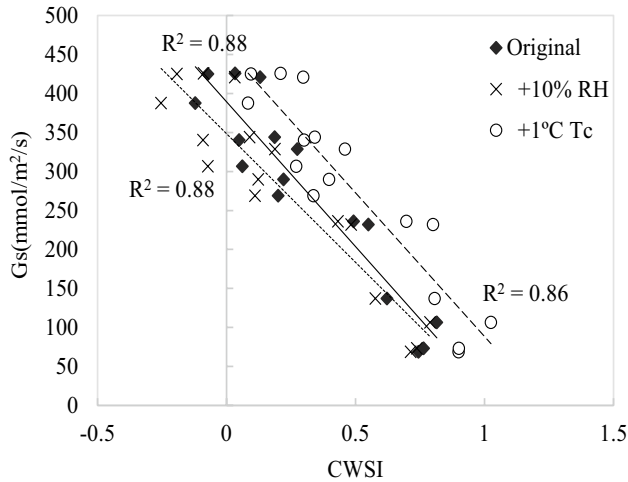
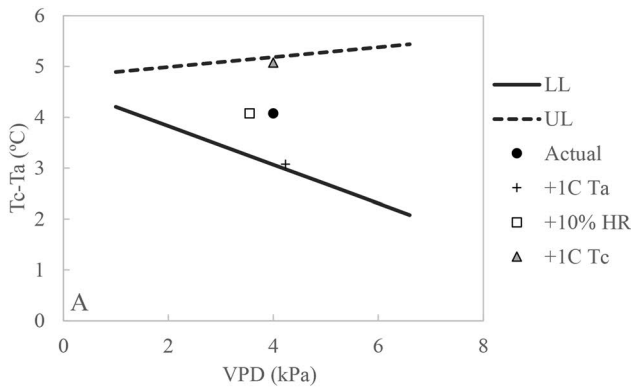


Fig. 8 Relationship between the CWSI and stomatal conductance for the original dataset (continuous line), and considering an error of +10% in RH (dotted line) and +1 °C in canopy temperature (discontinuous line)



between the upper and lower limits are often large. These species are decoupled to the atmosphere, and therefore, the transpiration is mainly determined by the radiation load.

From the three data inputs under study, T_a , T_c , and RH, the air temperature was the variable that displayed more significant effects, as it is involved in both, $T_c - T_a$ and VPD calculations. In squash crop, the studied error resulted in a variation of CWSI smaller than 10%, while it yielded 90% in orange. Inaccuracies in canopy temperature estimation also resulted in significant effects on the calculated CWSI. Relative humidity was the input that affected less to the overall calculation. For the three inputs, the effect was maximum for the minimum VPD considered in this study (2 kPa) and decreased as VPD raised.

The actual CWSI value slightly affected the magnitude of the error in the case of the temperature data (either air or canopy). Although of smaller absolute values, the effect of the relative humidity was dependent on the CWSI value. The magnitude of this error was maximal when the CWSI was close to 0, and it was equal to 0 for CWSI values of 1. Consequently, the relationship with physiological measures was not severely affected in relative terms, and the level of significance was maintained, but with contrasted absolute values.

This study highlights the relevance of accurate values of T_a and RH for the calculation of CWSI, and calibrated thermal sensors providing accurate canopy temperature in absolute terms. Errors of stomatal conductance close to $70\text{ mmol/m}^2/\text{s}$ can be obtained in the relationships between CWSI and G_s when the air temperature is obtained with $1\text{ }^{\circ}\text{C}$ error.

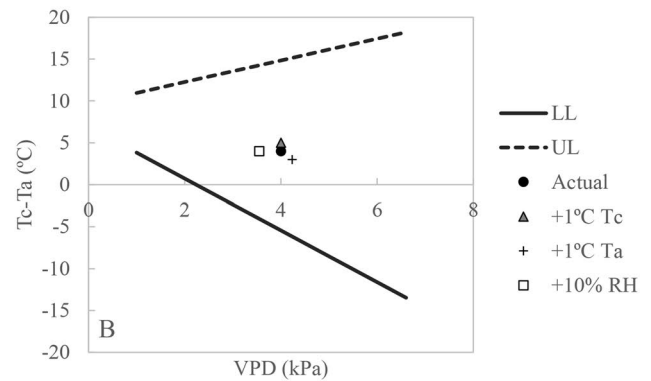


Fig. 9 Example of the displacement in actual values within the relationship between $T_c - T_a$ ($^{\circ}\text{C}$) and VPD (kPa) associated with an error of +1 °C T_a , +1 °C T_c , and +10%RH, in orange (A) and squash (B).

Lower and upper limits are plotted for both species. The value used as illustration corresponded with a VPD equal to 4 kPa and a CWSI of 0.5

Supplementary Information The online version contains supplementary material available at <https://doi.org/10.1007/s00271-022-00819-6>.

Acknowledgements The authors acknowledge Alberto Hornero, Alberto Vera, David Notario, and Rafa Romero for their technical support with imagery acquisition and processing and Dr. Lopez-Lopez for designing and managing the almond irrigation experiment.

Funding Open Access funding provided thanks to the CRUE-CSIC agreement with Springer Nature. The authors acknowledge the financial support from the Spanish Ministry of Science and Innovation (RTI2018-096754-J-100). Victoria Gonzalez-Dugo was supported by a postdoctoral grant, “Ramon y Cajal” (RYC2018-024994-I).

Declarations

Conflict of interest On behalf of all authors, the corresponding author states that there is no conflict of interest.

Open Access This article is licensed under a Creative Commons Attribution 4.0 International License, which permits use, sharing, adaptation, distribution and reproduction in any medium or format, as long as you give appropriate credit to the original author(s) and the source, provide a link to the Creative Commons licence, and indicate if changes were made. The images or other third party material in this article are included in the article's Creative Commons licence, unless indicated otherwise in a credit line to the material. If material is not included in the article's Creative Commons licence and your intended use is not permitted by statutory regulation or exceeds the permitted use, you will need to obtain permission directly from the copyright holder. To view a copy of this licence, visit <http://creativecommons.org/licenses/by/4.0/>.

References

- Agam N, Cohen Y, Alchanatis V, Ben-Gal A (2013) How sensitive is the CWSI to changes in solar radiation? *Int J Remote Sens* 34:6109–6120. <https://doi.org/10.1080/01431161.2013.793873>
- Allen RG, Tasumi M, Trezza R (2007) Satellite-based energy balance for mapping evapotranspiration with internalized calibration (METRIC)—model. *J Irrig Drain Eng* 133:380–394. [https://doi.org/10.1061/\(ASCE\)0733-9437\(2007\)133:4\(380\)](https://doi.org/10.1061/(ASCE)0733-9437(2007)133:4(380))
- Apolo-Apolo OE, Martínez-Guanter J, Pérez-Ruiz M, Egea G (2020) Design and assessment of new artificial reference surfaces for real time monitoring of crop water stress index in maize. *Agric Water Manage* 240:106304. <https://doi.org/10.1016/j.agwat.2020.106304>
- Aragon B, Johansen K, Parkes S et al (2020) A calibration procedure for field and uav-based uncooled thermal infrared instruments. *Sensors* 20(11):3316–3340. <https://doi.org/10.3390/s20113316>
- Berni JAJ, Zarco-Tejada PJ, Sepulcre-Cantó G et al (2009a) Mapping canopy conductance and CWSI in olive orchards using high resolution thermal remote sensing imagery. *Remote Sens Environ* 113:2380–2388. <https://doi.org/10.1016/j.rse.2009.06.018>
- Berni JAJ, Zarco-Tejada PJ, Suárez L, Fereres E (2009b) Thermal and narrowband multispectral remote sensing for vegetation monitoring from an unmanned aerial vehicle. *IEEE Trans Geosci Remote Sens* 47:722–738. <https://doi.org/10.1109/TGRS.2008.2010457>
- Carrow RNB (1989) Turfgrass irrigation scheduling by infrared thermometry. In: *Proceedings of the 1989 Georgia Water Resources Conference*. Athens, University of Georgia, pp 63–65
- Dzikiti S, Steppe K, Lemeur R, Milford JR (2007) Whole-tree level water balance and its implications on stomatal oscillations in orange trees [*Citrus sinensis* (L.) Osbeck] under natural climatic conditions. *J Exp Bot* 58(7):1893–1901. <https://doi.org/10.1093/jxb/erm023>
- Gates DM (1968) Transpiration and leaf temperature. *Annu Rev Plant Physiol* 19:211–238
- Gonzalez-Dugo V, Zarco-Tejada P, Berni JAJ et al (2012) Almond tree canopy temperature reveals intra-crown variability that is water stress-dependent. *Agric for Meteorol* 154–155:156. <https://doi.org/10.1016/j.agrformet.2011.11.004>
- Gonzalez-Dugo V, Zarco-Tejada PJ, Fereres E (2014) Applicability and limitations of using the crop water stress index as an indicator of water deficits in citrus orchards. *Agric for Meteorol* 198–199:94–104. <https://doi.org/10.1016/j.agrformet.2014.08.003>
- Gonzalez-Dugo V, Lopez-Lopez M, Espadafor M et al (2019) Transpiration from canopy temperature: implications for the assessment of crop yield in almond orchards. *Eur J Agron* 105:78–85. <https://doi.org/10.1016/j.eja.2019.01.010>
- Idso SB (1982) Non-water-stressed baselines: A key to measuring and interpreting plant water stress. *Agric Meteorol* 27:59–70. [https://doi.org/10.1016/0002-1571\(82\)90020-6](https://doi.org/10.1016/0002-1571(82)90020-6)
- Idso SB, Jackson RD, Pinter PJ Jr et al (1981) Normalizing the stress-degree-day parameter for environmental variability. *Agric Meteorol* 24:45–55. [https://doi.org/10.1016/0002-1571\(81\)90032-7](https://doi.org/10.1016/0002-1571(81)90032-7)
- Idso SB, Pinter PJ Jr, Reginato RJ (1990) Non-water-stressed baselines: the importance of site selection for air temperature and air vapour pressure deficit measurements. *Agric for Meteorol* 53:73–80. [https://doi.org/10.1016/0168-1923\(90\)90125-P](https://doi.org/10.1016/0168-1923(90)90125-P)
- Irmak S, Haman DZ, Bastug R (2000) Determination of crop water stress index for irrigation timing and yield estimation of corn. *Agron J* 92:1221–1227. <https://doi.org/10.2134/agronj2000.9261221x>
- Jackson RD, Reginato RJ, Idso SB (1977) Wheat canopy temperature: a practical tool for evaluating water requirements. *Water Resour Res* 13:651–656. <https://doi.org/10.1029/WR013i003p00651>
- Jarvis PG (1985) Coupling of transpiration to the atmosphere in horticultural crops: the omega factor. *Acta Hort* 171:187–206. <https://doi.org/10.17660/ActaHortic.1985.171.17>
- Jones HG (1999) Use of infrared thermometry for estimation of stomatal conductance as a possible aid to irrigation scheduling. *Agric for Meteorol* 95:139–149. [https://doi.org/10.1016/S068-1923\(99\)00030-1](https://doi.org/10.1016/S068-1923(99)00030-1)
- Jones HG, Stoll M, Santos T, de Sousa C, Chaves MM, Grant OM (2002) Use of infrared thermography for monitoring stomatal closure in the field: application to grapevine. *J Exp Bot* 53(378):2249–2260. <https://doi.org/10.1093/jxb/erf083>
- Khand K, Taghvaeian S, Hassan-Esfahani L (2017) Mapping annual riparian water use based on the single-satellite-scene approach. *Remote Sens*. <https://doi.org/10.3390/rs9080832>
- Leinonen I, Jones HG (2004) Combining thermal and visible imagery for estimating canopy temperature and identifying plant stress. *J Exp Bot* 55(401):1423–1431. <https://doi.org/10.1093/jxb/erh146>
- Lopardo G, Bellagarda S, Bertiglia F, Merlone A, Roggero G, Jandric N (2015) A calibration facility for automatic weather stations. *Meteorol Appl* 22:842–846. <https://doi.org/10.1002/met.1514>
- Lopes I, Guimarães MJM, de Melo JMM et al (2021) Comparison of meteorological data, related to reference evapotranspiration, from conventional and automatic stations in the sertão and agreste regions of pernambuco Brazil. *Comp Datos Meteorol Relacion Evapotransp DYNA* 88:176–183. <https://doi.org/10.15446/dyna.v88n216.86372>
- Maes WH, Steppe K (2012) Estimating evapotranspiration and drought stress with ground-based thermal remote sensing in agriculture: a review. *J Exp Bot* 63:4671–4712. <https://doi.org/10.1093/jxb/ers165>
- Maes WM, Baert A, Huete AR, Minchin PEH, Snelgar WP, Steppe K (2016) A new wet reference target method for continuous infrared

- thermography of vegetations. *Agric for Meteorol* 226–227:119–131. <https://doi.org/10.1016/j.agrformet.2016.05.021>
- Mason EG, Salekin S, Morgenroth JA (2017) Comparison between meteorological data from the New Zealand National Institute of Water and Atmospheric Research (NIWA) and data from independent meteorological stations. *New Zeal J for Sci*. <https://doi.org/10.1186/s40490-017-0088-0>
- Meron M, Tsipris J, Orlov V et al (2010) Crop water stress mapping for site-specific irrigation by thermal imagery and artificial reference surfaces. *Precis Agric* 11:148–162. <https://doi.org/10.1007/s11119-009-9153-x>
- Poirier-Pocovi M, Bailey BN (2020) Sensitivity analysis of four crop water stress indices to ambient environmental conditions and stomatal conductance. *Sci Hortic (amsterdam)*. <https://doi.org/10.1016/j.scienta.2019.108825>
- Sepulcre-Canto G, Zarco Tejada PJ, Jimenez-Muñoz JC, Sobrino JA, de Miguel E, Villalobos FJ (2006) Detection of water stress in olive orchard with thermal remote sensing imagery. *Agric for Met* 136:31–44. <https://doi.org/10.1016/j.agrformet.2006.01.008>
- Taghvaeian S, Chávez JL, Hansen NC (2012) Infrared thermometry to estimate crop water stress index and water use of irrigated maize in northeastern colorado. *Remote Sens* 4:3619–3637. <https://doi.org/10.3390/rs4113619>
- Testi L, Goldhamer DA, Iniesta F, Salinas M (2008) Crop water stress index is a sensitive water stress indicator in pistachio trees. *Irrig Sci* 26:395–405. <https://doi.org/10.1007/s00271-008-0104-5>
- Veste M, Ben-Gal A, Shani U (2000) Impact of thermal stress and high vpd on gas exchange and chlorophyll fluorescence of citrus grandis under desert conditions. *Acta Hortic* 531:143–150
- Villalobos FJ, Testi L, Moreno-Perez MF (2009) Evaporation and canopy conductance of citrus orchards. *Agric Water Manage* 96:565–573. <https://doi.org/10.1016/j.agwat.2008.09.016>
- World Meteorological Organization (2010) Guide to agricultural meteorological practices, second edition. Guide to Agric Meteorol Pract Second Ed 134
- Zhao T, Niu H, Anderson A et al (2018) A detailed study on the accuracy of uncooled thermal cameras by exploring the data collection workflow. In: Proc. SPIE 10664, autonomous air and ground sensing systems for agricultural optimization and phenotyping III, 106640F (21 May 2018). <https://doi.org/10.1117/12.2305217>

Publisher's Note Springer Nature remains neutral with regard to jurisdictional claims in published maps and institutional affiliations.